

35. RARE-GAS STUDIES OF CRETACEOUS DEEP-SEA BASALTS

Nobuo Takaoka and Keisuke Nagao, Department of Physics, Faculty of Science, Osaka University, Toyonaka-shi, Osaka-fu 560, Japan

ABSTRACT

The concentrations and isotopic ratios of rare gases were determined in glasses of the Cretaceous oceanic basalts drilled during Leg 51. Glasses from two samples are enriched in Ne relative to atmospheric rare gases. ^3He was detected in one sample. The $^3\text{He}/^4\text{He}$ ratio determined is $(3 \pm 1) \times 10^{-6}$. The $^{40}\text{Ar}/^{36}\text{Ar}$ ratio and Ar concentration at the proto-Bermuda Rise are compatible with modern glasses. The isotopic compositions of Ne, Kr, and Xe are atmospheric.

INTRODUCTION

Knowledge of the abundance and isotopic composition of rare gases in the mantle can provide important constraints on the study of the origin and evolution of the atmosphere. One of the sources of information on the rare-gas state of the mantle comes from basalts which erupted from oceanic ridges (Fisher, 1971). Several authors have reported that the quenched rims of deep-sea basalts contain excess ^4He and ^{40}Ar trapped when they erupted onto the ocean floor under great hydrostatic pressure (Fisher et al., 1968; Funkhouser et al., 1968; Dalrymple and Moore, 1968; Noble and Naughton, 1968; Fisher, 1971). From rare-gas studies of meteorites and lunar material, it is well known that there are two distinct types of primordial rare gases in the solar system: the solar and the planetary rare gases. Dymond and Hogan (1973) have reported rare-gas abundance patterns in glassy rims of oceanic basalts which show significant enrichment in light elements relative to the atmosphere and resemble the abundance pattern of the solar rare gases found in extra-terrestrial samples. They argued that the glassy rims of pillow basalts contain the primordial gases whose elemental abundance pattern resembles the solar gases. In a report on Ar, Kr, and Xe measurements in basalts dredged from several deep-sea locations, Fisher (1974) agreed that primordial rare gases are present in the glassy rims of oceanic basalts. However, he argued that the abundance pattern is planetary rather than solar.

Ozima and Alexander (1976) argued that the elemental composition of rare gases in the quenched rims might represent highly fractionated planetary primordial rare gases. They presented a model in which the fractionation was due to the differential diffusivity of the rare gases during the formation of the magma in the mantle. Since the fractionation depended on the difference in the atomic radii of the elements, the isotopic composition of the primordial rare gases would scarcely be affected by such a fractionation process.

Isotopic evidence for the presence of the primordial gases in oceanic basalts has been given by Lupton and Craig (1975) and Craig and Lupton (1976). They measured the

isotopic ratios of He and Ne in the glasses of oceanic basalts of relatively young ages, and found the $^3\text{He}/^4\text{He}$ ratio as high as 1.4×10^{-5} (an order of magnitude higher than the ratio of atmospheric He) and a slight enrichment in ^{20}Ne . In addition to He and Ne, the isotopic composition of Xe is useful in identifying the primordial component. However, there has been no data reported to date on the isotopic ratios of Xe in the glassy rims of pillow basalts, with the exception of Fisher (1974). He reported that the isotopic ratios of Xe were identical with the atmospheric ratios within a 5 percent error for the isotopes 129 to 136. To distinguish between atmospheric Xe and planetary and solar Xe, however, smaller errors and measurements of the light isotopes 124, 126, and 128 are necessary.

In this work, we report the result on the concentrations and isotopic compositions of rare gases in glassy rims of the Cretaceous pillow basalts, drilled near the southern end of the Bermuda Rise during the Deep Sea Drilling Project, Leg 51. This is the first measurement, including the elemental and isotopic compositions, of all the stable rare gases in oceanic crust older than 100 m.y. It gives useful information on the rare gas retention by quenched rims for 100 m.y., as well as the rare gas composition of the proto-Bermuda Rise event.

EXPERIMENTAL METHOD

Sample Description

Samples used in this work are from the glassy rims of the Cretaceous pillow basalt cores drilled in a re-entry Hole 417D of Leg 51. According to the Site 417 Chapter, Site 417 is on magnetic anomaly *M0* which has been estimated to be 108 m.y. old. Three samples from different cores (Samples 417-22-3, 24-27 cm; 417-28-5, 85-92 cm; and 417-29-6, 95-104 cm) were investigated for rare gases. According to the Site 417 Chapter, Core 22 is the highest core and is nearest to the top of the basement. Cores 28 and 29 are about 40 and 50 meters below Core 22, respectively. Cores 22 and 28 have been identified as plagioclase olivine-phyric pillow basalts. Core 29 is a plagioclase olivine clinopyroxene-phyric pillow basalt.

According to Ui (written communication, 1977), microscopic examination of thin sections of the same cores as used in this work shows that groundmass and crystals in glassy rim from Core 22 are surrounded by dark, partially altered glass and that there are many cracks in the glassy rim along which the alteration of glass is advanced. Gas pores have been filled with altered material in this core. For Core 28, the alteration of glass is so advanced that fresh glass is a minor component and large cracks have filled with altered minerals such as carbonate, clay, and zeolites. Glass from Core 29 is mostly fresh. The alteration of glass along cracks is less extensive; only the insides of large cracks have been filled with altered material. From a microscopic examination of thin sections, therefore, the alteration of glass is more advanced in the following sequence: Cores 29, 22, and 28.

All samples were supplied as slices of basalts with glassy rims attached. The glassy parts were crushed in a stainless steel mortar; glassy, lustrous, fresh fragments were carefully separated by hand-picking. Samples identified as 1, 3, and 5 consist of these separates; 0.4 to 0.6 gram fractions of these separates were wrapped with 10- μ m-thick aluminum foil (~25 mg). For precise determination of the isotopic composition, larger sample sizes were prepared. Samples designated as 2, 4, and 6 are glasses separated from the same slices from which 1, 3, and 5 were prepared, respectively. However, they may contain some altered material because of the larger sample size.

Mass Spectrometry

Experimental techniques used for the rare-gas analyses are essentially the same as described by Takaoka (1976). All samples were heated at about 100°C overnight in a vacuum to reduce atmospheric contamination. Sample 3 was heated at 700°C for 30 minutes and then melted at 1300°C for 30 minutes. To check for incomplete degassing Sample 3 was reheated at 1350°C for 30 minutes. Approximately 55 per cent of the He was released at 700°C, while 66 per cent of the Xe was released at 1300°C. In the 1350°C fraction, 8 per cent of Xe remained. Less than 0.02 per cent of He appeared in this fraction. Other gases were released at 700° and 1300°C in a similar pattern to that for He. The fractions remained in the 1350°C fraction were 0.2, 3, and 4 per cent of total amounts released for Ne, Ar, and Kr, respectively. Samples 1 and 5 were melted at 1500°C for 30 minutes. Samples 2, 4, and 6 were heated at 500°C for 30 minutes and then melted at 1500°C for 30 minutes. Parts of Sample 6 were caught in the middle of a tantalum crucible by a canopy of slag from the samples previously melted. They were taken out of the tantalum crucible and re-analyzed in a separate run. However, the atmospheric contamination on the sample made the precise determinations of both concentrations and isotopic ratios of rare gases (except He) difficult in the reheating run. For He in Sample 6, 67 per cent was released at 1500°C in the first run, and 31 per cent during reheating. $^3\text{He}/^4\text{He}$ ratios in both fractions of Sample 6 are practically identical.

The electron accelerating voltage in the ion source was set at 40 volt to reduce the influence of doubly charged ^{40}Ar

and CO_2 ions. The mass spectrometer was tuned to a mass resolution of about 600 by adjusting the width of a collector slit. With this resolution, the spectrometer can separate ^3He from H_3 and HD; and ^{38}Ar , ^{40}Ar , and all the isotopes of Kr and Xe from the isobaric hydrocarbon peaks. Separation between ^{20}Ne and H_2^{18}O is also fairly good. Before the sample analyses, blanks were run under the same conditions and procedures as applied to the sample gases. The concentrations of rare gases and the isotopic ratios of He, Ne, and Ar were corrected for the blank. The isotopic ratios of Kr and Xe were not corrected for the blank. The isotopic ratios of blank Kr and Xe were atmospheric. The rare gases evolved from the aluminum foil were corrected using the concentrations of rare gases in the aluminum foil. The concentrations of rare gases in the aluminum foil are: 6.6×10^{-10} for ^4He , 2.5×10^{-10} for ^{20}Ne , 7.0×10^{-11} for ^{36}Ar , 4.5×10^{-11} for ^{84}Kr , and 5.9×10^{-13} for ^{132}Xe in units of $\text{cm}^3\text{STP/gAl}$. Sensitivity and mass discrimination of the spectrometer, including the sampling system, were determined by measuring a known amount of air. The mass discrimination for $^3\text{He}/^4\text{He} = 1.32 \times 10^{-4}$ as later used to check reliability of the mass discrimination correction with the Bruderheim standard. No evidence was found for non-linearity of the spectrometer, which might arise from the great difference in abundance between ^3He and ^4He . Corrections for blanks including the aluminum foil were typically (in units of cm^3STP): $<1 \times 10^{-9}$ for ^4He , $<2 \times 10^{-11}$ for ^{20}Ne , $<3 \times 10^{-11}$ for ^{36}Ar , $<1 \times 10^{-12}$ for ^{84}Kr , and 1×10^{-13} for ^{132}Xe . The correction for $^{40}\text{Ar}^{++}$ in ^{20}Ne was less than 2 per cent. However, the correction for CO_2^{++} in ^{22}Ne was relatively high due to an accidentally high contamination of CO_2 in the analyses of the oceanic basalts. The correction often amounted to a few tens of per cent.

RESULTS AND DISCUSSION

Elemental Abundance

Table 1 shows the concentrations of the most abundant isotope of each rare-gas element in the glassy rims of the Cretaceous pillow basalts. The concentrations of gases show large variations even in samples prepared from the same slice of core. This means that there are great heterogeneities in the rare-gas abundances in the quenched rims. The cause is probably due to spotty alteration of glass as described earlier. The elemental abundance patterns relative to atmospheric gases are plotted in Figure 1. Enrichment in Ne is apparent in Samples 3 and 5. This confirms the enrichment in Ne discovered by Dymond and Hogan (1973) for the rare gases in glasses of deep-sea pillow basalts. Other samples are depleted in Ne and enriched in ^{36}Ar and Kr, compared with Samples 3 and 5. There is a trend that Kr is more depleted in the glasses of the Cretaceous basalts except for Sample 3, compared with the result for young pillow basalts given by Dymond and Hogan (1973).

Isotopic Composition

Part of the result on the isotopic ratios is compiled in Table 2. ^3He could be detected only in Sample 6. The $^3\text{He}/^4\text{He}$ ratio determined for Sample 6 is $3(\pm 1) \times 10^{-6}$.

TABLE 1
Concentrations of Rare Gases in Glasses of
Cretaceous Deep-Sea Basalts, Hole 417D

Sample	1	2	3	4	5	6
DSDP Core	22	22	28	28	29	29
Weight (g)	0.432	2.37	0.630	1.91	0.471	0.907
^4He (10^{-6} cm 3 /g)	0.567	1.32	1.10	0.698	1.06	2.23
^{20}Ne (10^{-9} cm 3 /g)	0.37	0.920	2.37	0.644	2.98	0.26
^{36}Ar (10^{-9} cm 3 /g)	1.44	2.14	1.65	4.42	0.998	5.95
^{84}Kr (10^{-11} cm 3 /g)	2.5	7.8	6.9	3.6	1.3	2.9
^{132}Xe (10^{-11} cm 3 /g)	0.918	0.930	1.1	1.22	0.258	0.58

Note: Because of the atmospheric contamination in the reheating run of Sample 6, Ne, Kr, and Xe which appeared in this run are not included. He and Ar which could be corrected for the atmospheric contamination are included in the concentration. The atmospheric contamination in He was about 1 per cent. The correction for atmospheric Ar is given by assuming that Ar released in the reheating run is a mixture of contaminating atmospheric Ar and sample Ar of the $^{40}\text{Ar}/^{36}\text{Ar}$ ratio (567) which was measured in the 1500°C fraction of the first run.

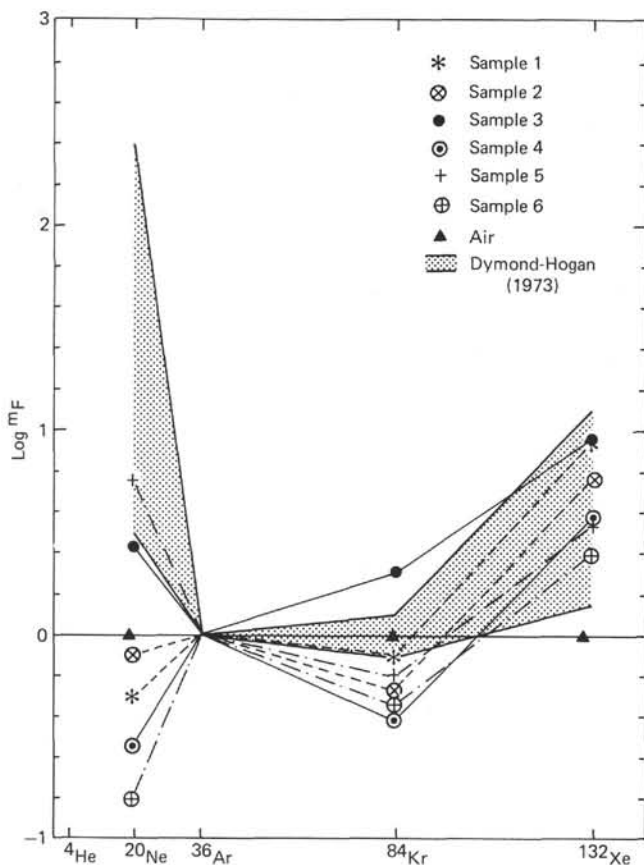


Figure 1. Elemental abundance pattern relative to atmospheric rare gases. Definition of m_F is given by: $m_F = \frac{(mX/^{36}\text{Ar})_{\text{sample}}}{(mX/^{36}\text{Ar})_{\text{atm}}}$.

Upper limits of the $^3\text{He}/^4\text{He}$ ratio for other samples were calculated with a detection limit for ^3He ($\sim 1 \times 10^{-12}$ cm 3 STP) and the amounts of ^4He determined. As mentioned earlier, Lupton and Craig (1975) and Craig and Lupton (1976) have reported $^3\text{He}/^4\text{He}$ ratios as high as 1.4×10^{-5} for glasses of young pillow basalts. They have also reported

$^3\text{He}/^4\text{He}$ ratios of 3.8 and 5.2×10^{-6} in the ~ 30 m.y.B.P. tholeiitic glass from Core 3 of Hole 320B drilled on Leg 34 between the Galapagos Rise and the Peru-Chile Trench. They attribute this low $^3\text{He}/^4\text{He}$ ratio to diffusive loss of He from the quenched glass. Applying a slab diffusion model (Craig and Lupton, 1976) to the present result, 100 m.y. is long enough for He to diffuse from a slab with a width of 2 cm with the diffusion coefficient of $D = 5 \times 10^{-15}$ cm 2 /sec as given by Craig and Lupton (1976). Thus, the concentration of ^3He would be decreased below our detection limit unless the initial concentration of ^3He was inadmissibly high (7×10^{-7} cm 3 STP/g), or provided there was no additional supply of ^3He into glass. Detection of ^3He in Sample 6 shows that a detectable amount of ^3He still remains in the glass pillow basalt which had been buried in the oceanic crust of 100 m.y.

Isotopic ratios of Ne were atmospheric within experimental errors. Isotopic ratio $^{38}\text{Ar}/^{36}\text{Ar}$ is atmospheric except for Sample 1, for which the ratio is 0.194 ± 0.002 . The $^{40}\text{Ar}/^{36}\text{Ar}$ ratios are 1340, 1100, and 1690 for Samples 1, 3, and 5, respectively, while Samples 2, 4, and 6 give lower ratios of 819, 557, and 567, respectively. Ar data on the isotopic ratios for Sample 6 are from the 1500°C fraction in the first run. The $^{40}\text{Ar}/^{36}\text{Ar}$ ratio in the reheating run is $311 (\pm 3)$ showing heavy atmospheric contamination.

Using a model of mixing a given mantle component of Ar with atmospheric Ar, Dymond and Hogan (1978) have used a plot of $^{40}\text{Ar}/^{36}\text{Ar}$ versus $1/^{36}\text{Ar}$ to determine whether the $^{40}\text{Ar}/^{36}\text{Ar}$ ratios measured in glassy deep-sea basalts reflect the variability of this ratio in the mantle or whether the variation in $^{40}\text{Ar}/^{36}\text{Ar}$ ratios is due to dilution of a mantle component of Ar with an atmospheric component. On such a plot, data will fall along a straight line,

$$\left(\frac{^{40}\text{Ar}}{^{36}\text{Ar}}\right)_{\text{meas}} = \frac{(^{40}\text{Ar})_{\text{mantle}} + \text{rad} - (^{36}\text{Ar})_{\text{mantle}} \left(\frac{^{40}\text{Ar}}{^{36}\text{Ar}}\right)_{\text{atm}} + (^{40}\text{Ar}/^{36}\text{Ar})_{\text{atm}}}{(^{36}\text{Ar})_{\text{meas}}}$$

if the concentrations of mantle Ar and radiogenic ^{40}Ar are homogeneous in all the samples investigated. The equation given above is different from that given by Dymond and Hogan (1978). One of the differences is due to the presence of radiogenic ^{40}Ar produced by the *in situ* decay of ^{40}K in the 100-m.y.-old basaltic glasses, and another is due to an incomplete formulation of Equation 3 given by Dymond and Hogan (1978). Their Equation 3 includes the ratio of $(^{36}\text{Ar})_{\text{mantle}}$ to $(^{36}\text{Ar})_{\text{atm}}$ in the second term of the right side. The complete formulation of the model of mixing uniform concentrations of mantle Ar and radiogenic ^{40}Ar with variable amounts of atmospheric Ar results in the equation given in this work. Hence, no matter whether $(^{36}\text{Ar})_{\text{mantle}} \gg (^{36}\text{Ar})_{\text{atm}}$ or not, a plot of $(^{40}\text{Ar}/^{36}\text{Ar})_{\text{meas}}$ versus $(1/^{36}\text{Ar})_{\text{meas}}$ is linear with an intercept equal to $(^{40}\text{Ar}/^{36}\text{Ar})_{\text{atm}}$, and a slope is equal to $(^{40}\text{Ar})_{\text{mantle}} + \text{rad} - (^{36}\text{Ar})_{\text{mantle}} \cdot (^{40}\text{Ar}/^{36}\text{Ar})_{\text{atm}}$.

Figure 2 is the plot of $^{40}\text{Ar}/^{36}\text{Ar}$ versus $1/^{36}\text{Ar}$ for the Cretaceous deep-sea basalts. It defines a correlation line between correlation lines for modern deep-sea basalts given by Dymond and Hogan (1978). An intercept with the ordinate is 257 ± 69 , compatible with the atmospheric $^{40}\text{Ar}/^{36}\text{Ar}$ ratio (295.5). This indicates that the relatively

TABLE 2
Isotopic Ratios of Rare Gases in Glasses of the Cretaceous Pillow Basalts, Hole 417D

Sample	1	2	3	4	5	6 ^a
³ He/ ⁴ He	<1 × 10 ⁻⁶	<2 × 10 ⁻⁶	<7 × 10 ⁻⁶	<2 × 10 ⁻⁶	<5 × 10 ⁻⁶	(3 ± 1) × 10 ⁻⁶
⁴⁰ Ar/ ³⁶ Ar	1341 ± 7	819 ± 22	1103 ± 7	557 ± 7	1686 ± 11	567 ± 17
¹²⁴ Xe/ ¹³² Xe	—	0.0034 ± 0.0004	—	0.0037 ± 0.0003	—	0.0037 ± 0.0005
¹²⁶ Xe/ ¹³² Xe	—	0.0032 ± 0.0003	—	0.0036 ± 0.0002	—	0.0034 ± 0.0006
¹²⁸ Xe/ ¹³² Xe	—	0.0716 ± 0.0026	—	0.0698 ± 0.0021	—	0.0715 ± 0.0033
¹²⁹ Xe/ ¹³² Xe	—	0.981 ± 0.009	—	0.988 ± 0.009	—	0.986 ± 0.013
¹³⁰ Xe/ ¹³² Xe	—	0.152 ± 0.003	—	0.153 ± 0.002	—	0.151 ± 0.003
¹³¹ Xe/ ¹³² Xe	—	0.788 ± 0.009	—	0.786 ± 0.008	—	0.799 ± 0.010
¹³⁴ Xe/ ¹³² Xe	—	0.390 ± 0.004	—	0.388 ± 0.005	—	0.389 ± 0.008
¹³⁶ Xe/ ¹³² Xe	—	0.334 ± 0.006	—	0.332 ± 0.006	—	0.339 ± 0.009

^aData in 1500°C fraction are given except ³He/⁴He which is the sum of the 500 and 1500°C fractions and remelt (see text).

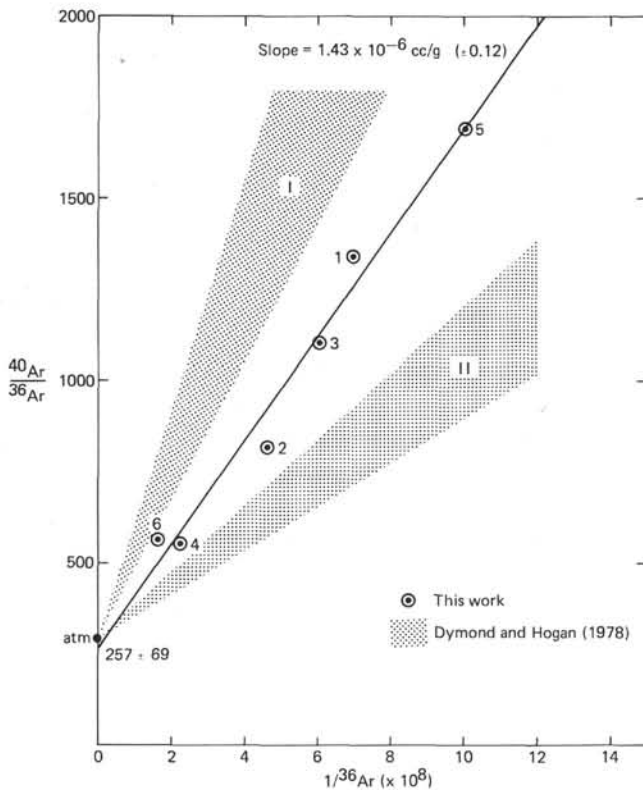


Figure 2. ⁴⁰Ar/³⁶Ar versus 1/³⁶Ar plot for the Cretaceous deep-sea basalts, Site 417. Shaded parts represent scattering about correlation lines for modern deep-sea basalts given by Dymond and Hogan (1978). Ar data for the Cretaceous basalts define a correlation line between the modern basalts. An intercept with the ordinate is 257 ± 69, compatible with the atmospheric ⁴⁰Ar/³⁶Ar ratio (295.5). The linear correlation strongly suggests uniform concentrations of mantle Ar and radiogenic ⁴⁰Ar in the Cretaceous basalts which were mixed with different amounts of atmospheric Ar. Correction for radiogenic ⁴⁰Ar brings the correlation line near the correlation line (II) for the modern basalts.

uniform concentrations of mantle ³⁶Ar and ⁴⁰Ar, and radiogenic ⁴⁰Ar produced by the *in situ* decay of ⁴⁰K were mixed with variable amounts of atmospheric Ar. Sample 5 which was prepared from Core 29 shows the least contamination on this plot. Sample 1 from Core 22 and Sample 3 from Core 28 are more contaminated in that sequence. This sequence for atmospheric contamination is in good agreement with that for the alteration of glass determined from the microscopic examination of the thin sections of the same cores (Ui, written communication, 1977).

Potassium concentration in the present samples was not measured. However, according to Ui et al. (this volume), the potassium concentration has been determined in basaltic glasses from the same cores as used in this work. The potassium concentration is 0.083, 0.091 and 0.075 weight per cent for Samples 22-3, 24-27 cm; 28-5, 85-92 cm; and 29-6, 95-104 cm, respectively. Radiogenic ⁴⁰Ar was corrected with these values of potassium and the age of 100 m.y.B.P. Typically, 3.5 × 10⁻⁷ cm³STP/g of ⁴⁰Ar is attributed to radiogenic ⁴⁰Ar produced in the basaltic glass during the past 100 m.y. The correction for the atmospheric contamination is difficult. Craig and Lupton (1976) have adopted an average of 0.5 × 10⁻⁹ cm³/g for ³⁶Ar initially trapped in young unaltered glass. In this case, most of the ³⁶Ar measured is attributed to the atmospheric contamination. Another assumption, which is an extreme and unpractical case, is no atmospheric contamination. In this case, all ³⁶Ar is trapped initial Ar. Table 3 shows the initial (or excess) amounts of ⁴⁰Ar and the initial ⁴⁰Ar/³⁶Ar ratios estimated from these two different assumptions. The absolute amounts of excess ⁴⁰Ar are reasonably constant and are independent of the atmospheric correction, especially in Samples 1, 3, and 5, and are in agreement with literature values of 0.01 to 3 × 10⁻⁶ cm³/g for glasses of young oceanic basalts (Funkhouser et al., 1968; Darlymple and Moore, 1968; Noble and Naughton, 1968; Fisher, 1971; Dymond and Hogan, 1973; Fisher, 1975). On the other hand, the initial ⁴⁰Ar/³⁶Ar ratio depends critically on the correction for atmospheric Ar. However, the ratio is constant around 2400 for Samples 1, 3, and 5 which are the glass separates prepared from three different cores (22, 28,

TABLE 3
Estimation of the Amount of Initial ^{40}Ar and of the Initial $^{40}\text{Ar}/^{36}\text{Ar}$ Ratios,
Trapped in the Hole 417D Cretaceous Basaltic Glasses at the Proto-Bermuda Rise Event

Sample Assumption	1		2		3		4		5		6	
	A	B	A	B	A	B	A	B	A	B	A	B
$^{40}\text{Ar}(10^{-6} \text{ cm}^3/\text{g})$	1.3	1.6	0.92	1.4	1.1	1.5	0.93	2.1	1.2	1.4	1.5	3.1
$^{40}\text{Ar}/^{36}\text{Ar}$	2600	1100	1800	660	2200	880	1900	470	2500	1380	2900	520

Note: For assumption A, the initial ^{36}Ar was assumed to be $0.5 \times 10^{-9} \text{ cm}^3/\text{g}$ (Craig and Lupton, 1976) and the remaining ^{36}Ar attributed to atmospheric contamination; for assumption B, all of ^{36}Ar measured was assumed to be initial. In both cases, radiogenic ^{40}Ar was corrected.

and 29, respectively). This ratio is also in the range of the $^{40}\text{Ar}/^{36}\text{Ar}$ ratio found in glasses of young oceanic basalts (Dymond and Hogan, 1973; Fisher, 1975).

The isotopic composition of Kr was atmospheric. The isotopic ratios of Xe are listed in Table 2 for Samples 2, 4, and 6. Data for Sample 6 are those given in the 1500°C fraction of the first run and do not include data in the reheating run because of heavy atmospheric contamination. The isotopic ratios of Xe for Samples 1, 3, and 5 were less reliable due to the small sample size. Figure 3 shows the fractional excess patterns relative to atmospheric Xe. The excess patterns for Samples 1, 3, and 5 were atmospheric within experimental errors. AVCC-Xe (Eugster et al., 1967) and solar Xe (Podosek et al., 1971) are also plotted. The definition of the fractional excess is given by

$$\delta^{132}(\text{m}) = \left\{ \frac{(^m\text{Xe}/^{132}\text{Xe})_{\text{sample}}}{(^m\text{Xe}/^{132}\text{Xe})_{\text{atmosphere}}} - 1 \right\} \times 1000 \text{ (in per mil)}$$

From Figure 3, the isotopic composition of Xe in the Cretaceous basalts resembles neither AVCC-Xe nor solar Xe; rather it resembles atmospheric Xe. An upper limit of mixing of AVCC-Xe is estimated. Dotted lines in Figure 3 represent the excess patterns when 10 and 30 percent of AVCC-Xe are mixed with atmospheric Xe, respectively. Comparison between the present result on the Xe isotopic ratios and the calculated excess patterns given in Figure 3 rejects more than 30 per cent mixing of AVCC-Xe in the Cretaceous oceanic basalt glasses.

CONCLUSIONS

1. The concentrations and isotopic compositions were determined of all the stable rare gases. ^3He was detected in one sample of rapidly quenched glass. The $^3\text{He}/^4\text{He}$ ratio is $3(\pm 1) \times 10^{-6}$. Enrichment in Ne relative to atmospheric rare gases was found in separates of fresh glasses.

2. Ar data represent a linear correlation on the plot of $^{40}\text{Ar}/^{36}\text{Ar}$ versus $1/^{36}\text{Ar}$, which suggests a mixing of the relatively uniform concentration of trapped mantle Ar and of radiogenic ^{40}Ar with variable amounts of atmospheric Ar. The concentration of mantle (or excess) ^{40}Ar and the $^{40}\text{Ar}/^{36}\text{Ar}$ ratio of mantle Ar trapped for the proto-Bermuda Rise are compatible with those for the modern oceanic basalts. From these results, the rare gases seem to have been retained stably in the glassy rims during 100 m.y.

3. The isotopic compositions of Ne, Kr, and Xe were indistinguishable from the atmospheric ones. To identify the type of the primordial component in the mantle, precise

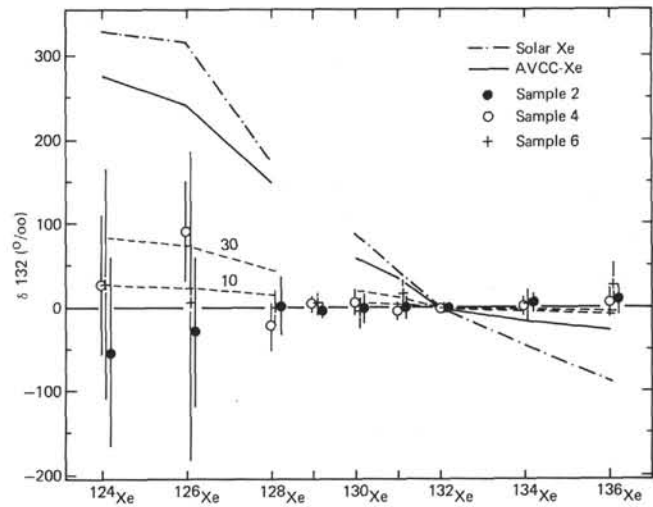


Figure 3. Fractional excess pattern of Xe in the Cretaceous basaltic glasses, Site 417. $\delta^{132}(\text{m})$ is defined by $\delta^{132}(\text{m}) = \left\{ \frac{(^m\text{Xe}/^{132}\text{Xe})_{\text{sample}}}{(^m\text{Xe}/^{132}\text{Xe})_{\text{atm}}} - 1 \right\} \times 1000 \text{ (in per mil)}$. Numerical figures on dotted lines represent percentage of AVCC-Xe mixing with atmospheric Xe.

determination of isotopic compositions of Ne and Xe is required in fresh samples which show the isotopic anomaly in He and the elemental enrichment in Ne.

ACKNOWLEDGMENTS

The authors express their sincere thanks to Prof. M. Ozima, Tokyo, for valuable comments and review of the manuscript, and for providing for the samples used in this work. They thank Drs. L. Hogan and R. Hart, Oregon, and Dr. I. Kaneoka, Tokyo, for many useful comments on the manuscript. The manuscript was edited for readability by Prof. E.C. Alexander, Jr., Minnesota. The authors are greatly indebted to Dr. T. Ui, Kobe, for permission to use unpublished data on the microscopic examination of thin sections and on the potassium content in the glasses from the same core samples as used in this work.

REFERENCES

- Craig, H. and Lupton, J.E., 1976. Primordial neon, helium, and hydrogen in oceanic basalts, *Earth Planet. Sci. Lett.*, v. 31, p. 369-385.
- Dalrymple, G.B. and Moore, J.G., 1968. Argon-40: excess in submarine pillow basalts from Kilauea Volcano, Hawaii, *Science*, v. 161, p. 1132-1135.

- Dymond, J. and Hogan, L. 1973. Noble gas abundance patterns in deep-sea basalts-primordial gases from the mantle, *Earth Planet. Sci. Lett.*, v. 20, p. 131-139.
- _____, 1978. Factors controlling the noble gas abundance patterns of deep-sea basalts, *Earth Planet. Sci. Lett.*, v. 38, p. 117-128.
- Eugster, O., Eberhardt, P., and Geiss, J., 1967. Krypton and xenon isotopic composition in three carbonaceous chondrites, *Earth Planet. Sci. Letter.*, v. 3, p. 249-257.
- Fisher, D.E., 1971. Incorporation of Ar in east Pacific basalts, *Earth Planet. Sci. Lett.*, v. 12, p. 321-324.
- _____, 1974. The planetary primordial component of rare gases in the deep earth, *Geophys. Res. Lett.*, v. 1, p. 161-164.
- _____, 1975. Trapped helium and argon and the formation of the atmosphere by degassing, *Nature*, v. 256, p. 113-114.
- Fisher, D.E., Bonatti, E., Joensuu, O., and Funkhouser, J., 1968. Ages of Pacific deep-sea basalts, and spreading of the sea floor, *Science*, v. 160, p. 1106-1107.
- Funkhouser, J.G., Fisher, D.E., and Bonatti, E., 1968. Excess argon in deep-sea rocks, *Earth Planet. Sci. Lett.*, v. 5, p. 95-100.
- Lupton, J.E. and Craig, H., 1975. Excess ^3He in oceanic basalts: evidence for terrestrial primordial helium, *Earth Planet. Sci. Lett.*, v. 26, p. 133-139.
- Noble, C.S. and Naughton, J.J. 1968. Deep-ocean basalts: inert gas content and uncertainties in age dating, *Science*, v. 162, p. 265-267.
- Ozima, M. and Alexander, E.C., Jr., 1976. Rare gas fractionation patterns in terrestrial samples and the earth-atmosphere evolution model, *Rev. Geophys. Space Phys.*, v. 14, p. 385-390.
- Podosek, F.A., Huneke, J.C., Burnett, D.S., and Wasserburg, G.J., 1971. Isotopic composition of xenon and krypton in the lunar soil and in the solar wind, *Earth Planet. Sci. Lett.*, v. 10, p. 199-216.
- Takaoka, N., 1976. A low-blank metal system for rare gas analysis, *Mass Spectroscopy*, v. 24, p. 73-86.